Experimental determination and modelling of high-pressure phase behavior for the binary system CO2 + cyclooctane

Stéphane Vitu, Andrés Piña-Martinez, Romain Privat, Marie Debacq, Jean-Louis Havet, Jean-Luc Daridon, Jean-Noël Jaubert

Experimental determination and modelling of high-pressure phase behavior for the binary system CO_2 + cyclooctane

Stéphane VITU [a,b], Andrés PIÑA-MARTINEZ [c], Romain PRIVAT [c], Marie DEBACQ [a,b],
Jean-Louis HAVET [a,b], Jean-Luc DARIDON [d], Jean-Noël JAUBERT [c,*]

[a] *Université Paris-Saclay, INRAE, AgroParisTech, UMR SayFood, 91300 Massy, France.*

[b] *CNAM, 2 rue Conté, 75003 Paris, France.*

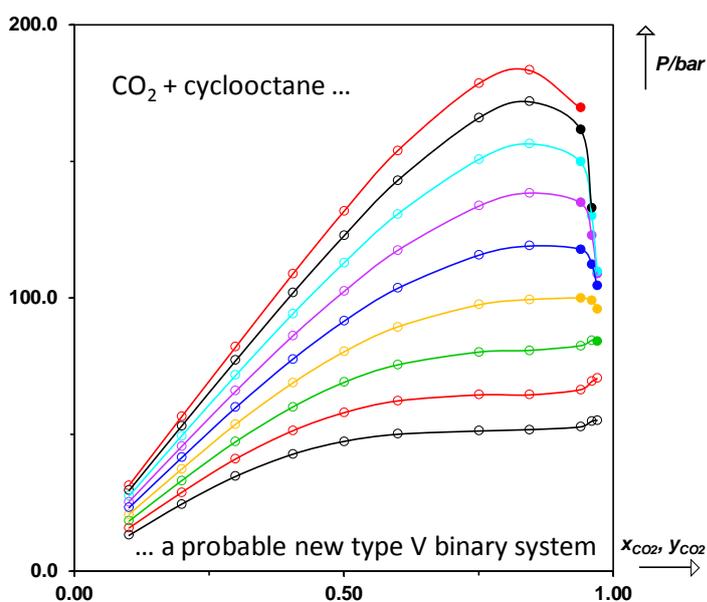[c] *Université de Lorraine, Ecole Nationale Supérieure des Industries Chimiques, Laboratoire Réactions et Génie des Procédés, 1 rue Grandville, 54000 Nancy, France.*

[d] *Université de Pau et des Pays de l'Adour, Laboratoire des Fluides Complexes et leurs Réservoirs, 64000 Pau, France.*

* Corresponding author.

E-mail: Jean-Noel.Jaubert@univ-lorraine.fr

Graphical Abstract:

Highlights

- High-pressure phase equilibria were measured for the system CO_2 + cyclooctane
- 80 bubble points and 16 dew points were acquired
- The experimental data were obtained using a variable volume high-pressure cell
- The studied binary system probably exhibits a type V phase behavior
- Data were correlated with the Peng-Robinson equation and advanced mixing rules

Abstract

Using a synthetic method, the phase behavior of the CO_2 (1) + cyclooctane (2) binary system was for the first time experimentally studied between 292.95 K and 373.55 K. In this temperature range, the bubble- and dew-point pressures, ranging from 13.2 to 183.4 bar were measured for carbon dioxide mole fractions between 0.1014 and 0.9701. A total of 96 experimental data points were acquired. The experimental data were obtained using a high-pressure cell by visual observation of phase transitions. These measurements made it possible to conclude that the studied binary system probably exhibits a type V phase behavior in the classification scheme of Van Konynenburg and Scott. In particular, the experimental temperature of the suspected lower critical end point (LCEP) was found to be 303 K. Despite the complexity of the phase behavior, the experimental data could be accurately correlated with the Peng-Robinson equation of state combined with sophisticated mixing rules that either involve temperature-dependent binary interaction parameters ($k_{ij}(T)$) or that embed the residual part of the Wilson activity coefficient model.

1. Introduction

The continuous increase of research articles devoted to high-pressure phase equilibria during the last 35 years shows the vitality of the supercritical fluid domain and the development of high-pressure processes [1,2]. Among these numerous papers, CO_2 remains the pure compound that is involved the most often in the investigated binary, ternary or more complex mixtures [3–7], especially because it is widely used in supercritical fluid separation processes. CO_2 is also a major greenhouse gas, and one of the technologies implemented to achieve carbon neutrality is the gas injection technique using captured CO_2, which is now routinely employed, not only to enhance oil recovery, but also to geologically store the CO_2. Phase equilibrium data of mixtures containing carbon dioxide are therefore still needed to design and improve industrial operations as well as to estimate the parameters of thermodynamic models [8–10].

Binary mixtures containing CO_2 and a hydrocarbon have been extensively measured and a vast amount of data involving a *basic* naphthene or aromatic component such as benzene, toluene, xylene, cyclopentane or cyclohexane are available [11,12]. However, a lack of data is observed for systems containing less common compounds. As an example, although experimental phase equilibrium data for the CO_2 + cyclopentane and CO_2 + cyclohexane binary systems are rather abundant, to the best of our knowledge, no experimental data were published for the binary system CO_2 + cycloheptane. For the CO_2 + cyclooctane system, only 3 solubility data at atmospheric pressure have been reported [13]. Broadly speaking, phase equilibrium data of mixtures involving a naphthenic compound that contains more than 6 carbon atoms in its ring are extremely scarce [11,14].

The objective of this study is to obtain new experimental vapor-liquid equilibrium (VLE) data for the system CO_2 (1) + cyclooctane (2) at high pressure. The experiments were conducted in a high-pressure cell with a sapphire window enabling direct observation of the phase transition. The experimental results were correlated with the Peng-Robinson (PR) equation of state (EoS) [15,16] armed with advanced mixing rules (MR) [17–19].

2. Experimental section

2.1. Materials

The carbon dioxide used in this study was supplied by Messer France and had a mass fraction purity higher than 0.999. Cyclooctane was supplied by Aldrich with a molar fraction purity higher than 0.990 and was used without any further purification.

2.2. Apparatus and procedure

Bubble and dew pressures were measured using a variable volume high-pressure cell. More details concerning the equipment used and the method can be found in our previous papers [20–22]. Briefly, the technique used to carry out vapor–liquid equilibrium measurements was based on a synthetic method (Synthetic-visual method with Variable-volume cell, "SynVisVar" according to Dohrn et al. [1,2]) which avoids sampling and analyses of both phases.

The experimental apparatus consisted of a stainless steel high-pressure cell with variable volume marketed by Top Industrie S.A.. One end of the cell was closed by a movable piston and the other end by a sapphire window allowing a visual observation of the equilibrium cell. A second sapphire window was fixed on the cylinder wall in order to illuminate the fluid with an optical fiber. Visualization was possible through the use of an endoscope placed right in front of the window.

The mixture was permanently homogenized thanks to a small magnetic bar and an external magnetic stirrer. The cell volume could be varied between 8 and 30 cm^3 and the internal temperature was kept constant by circulating a thermo–regulated heat–carrier fluid through three lines in the cell.

The temperature was precisely measured with a thermometer (AOIP brand, accuracy of 0.1 K) connected to a calibrated platinum resistance inserted into the cell, while pressure was measured by a piezoresistive-silicon pressure transducer (Kulite) directly placed inside the cell to minimize dead volumes. For each investigated temperature ranging from 293.15 K to 373.15 K, calibration of the pressure transducer was carried out between 0.1 and 100 MPa by means of a dead–weight gauge (Budenberg) with an accuracy of 0.02 %.

The equilibrium cell was first loaded with a known amount of cyclooctane by vacuum extraction. The exact mass of liquid introduced in the cell was determined using a precision balance (Ohaus) with an accuracy of 0.0001 g. CO_2 was then added under pressure. For this purpose, the gas was initially loaded onto a light weight tank fixed on the plate of a high mass / high precision balance (Sartorius). The maximum weighing capacity of this balance was

2000 g whereas its accuracy was 0.001 g. The CO_2 reservoir tank was connected to the cell by a flexible high-pressure capillary. The exact mass of CO_2 injected in the cell was thus determined by weighing the reservoir tank during the filling. Once done, the molar composition of the binary mixture contained in the cell (i.e. CO_2 + cyclooctane) could be straightforwardly calculated. From this procedure, the standard uncertainties in mass introduced were estimated to be lower than 0.01 g for liquid cyclooctane and 0.005 g for CO_2. When the desired temperature cell was reached, the pressure was slowly increased until the system became homogeneous. Due to supersaturation effects, the phase boundaries were evaluated by determining the disappearance conditions of one phase instead of its appearance meaning that measurements were carried out by observing the disappearance of the vapor phase (for a bubble point-pressure measurement) or the liquid phase (for a dew-point pressure measurement) at constant temperature. The method consisted first in observing the formation of a new phase by gradually changing the pressure and then reversing the direction of this variation in a stepwise fashion so as to detect the disappearance of the last phase formed. The procedure was repeated five times by reducing the increment. By doing so, reproducibility of the measured pressure at which the phase disappeared was 0.2 bar for bubble point pressure and 0.4 for dew point pressure while temperature was measured with an accuracy of 0.1 K.

3. Experimental results

For 11 different global compositions ranging from 0.1014 to 0.9701 CO_2 mole fraction, a total of 80 bubble-point pressures and temperatures and 16 upper dew point pressures and temperatures were experimentally measured for the CO_2 + cyclooctane binary system. Lower dew-point pressures were expected to be extremely small for the studied binary system so that it was not tried to measure them. The results are recorded in Table 1 for the 11 isopleths.

Table 1. Experimental bubble-point and dew-point pressures and temperatures for the CO_2 + cyclooctane binary mixture at 11 different CO_2 mole fractions as well as the uncertainties [a,b].

$x_{CO2} = 0.1014 \pm 0.0011$		$x_{CO2} = 0.1990 \pm 0.0010$		$x_{CO2} = 0.2996 \pm 0.0008$		$x_{CO2} = 0.4055 \pm 0.0008$		$x_{CO2} = 0.5007 \pm 0.0007$		$x_{CO2} = 0.6000 \pm 0.0005$	
T/K	P/bar	T/K	P/bar	T/K	P/bar	T/K	P/bar	T/K	P/bar	T/K	P/bar
293.05	13.2	293.15	24.5	293.15	34.7	292.95	42.6	293.25	47.6	293.05	50.0
302.45	15.5	302.45	28.5	302.65	40.7	302.45	50.9	302.65	57.5	302.75	61.8
312.65	18.2	313.15	33.0	312.45	47.1	312.35	59.3	312.75	68.5	312.65	74.7
323.15	20.8	323.25	37.4	322.55	53.3	322.35	68.2	322.65	79.8	322.85	88.9
332.55	23.1	332.65	41.4	332.75	59.7	332.55	77.0	333.05	91.4	333.05	103.4
342.65	25.3	342.65	45.3	342.35	65.5	343.15	86.1	343.15	102.5	343.05	117.4
352.75	27.4	352.85	49.3	352.55	71.3	352.55	93.9	353.05	112.7	352.95	130.4
362.95	29.5	362.65	53.0	362.65	76.8	362.65	101.3	362.85	122.6	362.75	142.5
373.45	31.5	372.35	56.2	372.65	81.9	373.15	108.9	373.15	131.8	373.25	154.1

$x_{CO2} = 0.7515 \pm 0.0007$		$x_{CO2} = 0.8445 \pm 0.0005$		$x_{CO2} = 0.9393 \pm 0.0004$		$x_{CO2} = 0.9602 \pm 0.0002$		$x_{CO2} = 0.9701 \pm 0.0002$	
T/K	P/bar	T/K	P/bar	T/K	P/bar	T/K	P/bar	T/K	P/bar
293.05	51.2	293.25	51.7	292.95	52.5	293.05	54.7	293.25	55.4
303.05	64.5	302.85	64.7	303.05	66.5	303.15	69.5	303.35	70.6
312.95	79.7	312.65	79.8	312.65	81.7	313.25	84.8	**312.95**	**84.1**
322.95	96.8	322.95	98.1	**323.05**	**99.0**	**322.95**	**98.3**	**322.95**	**95.3**
333.15	115.9	333.05	119.2	**332.85**	**117.7**	**333.05**	**112.4**	**333.15**	**104.7**
343.45	134.8	342.85	138.6	**342.65**	**134.6**	**343.05**	**122.9**	**342.85**	**108.5**
353.35	151.0	353.05	156.2	**353.75**	**150.4**	**353.15**	**129.7**	**353.05**	**109.7**
363.35	165.7	363.05	171.1	**363.25**	**161.2**	**362.95**	**133.1**		
373.55	179.3	372.95	183.4	**373.15**	**169.9**				

[a] Bold data are dew points; the rest are bubble points.
[b] Standard uncertainties u are u(T) = 0.1 K and u(P) = 0.2 bar for bubble points and u(P) = 0.4 bar for dew points.

Using a Microsoft Excel type solver, bubble and dew curves for constant composition can be approximated by polynomials from which isothermal P-x-y sections can be calculated at any temperature in the investigated temperature range. For nine temperatures ranging from 293.15 K to 373.15 K with a step of 10 K, isothermal (P,x,y) data obtained from the original measurements are given in Table 2 and are shown in Fig. 1.

Table 2. Isothermal (P,x,y) data for the CO_2 + cyclooctane binary system at nine different temperatures calculated from the original measurements reported in Table 1.

T/K = 293.15			T/K = 303.15			T/K = 313.15			T/K = 323.15			T/K = 333.15		
P/bar	x_{CO_2}	y_{CO_2}	P/bar	x_{CO_2}	y_{CO_2}	P/bar	x_{CO_2}	y_{CO_2}	P/bar	x_{CO_2}	y_{CO_2}	P/bar	x_{CO_2}	y_{CO_2}
13.1	0.1014	-	15.8	0.1014	-	18.3	0.1014	-	20.8	0.1014	-	23.2	0.1014	-
24.5	0.1990	-	28.8	0.1990	-	33.1	0.1990	-	37.3	0.1990	-	41.5	0.1990	-
34.7	0.2996	-	41.1	0.2996	-	47.4	0.2996	-	53.8	0.2996	-	59.9	0.2996	-
42.8	0.4055	-	51.4	0.4055	-	60.1	0.4055	-	68.9	0.4055	-	77.6	0.4055	-
47.5	0.5007	-	58.0	0.5007	-	69.1	0.5007	-	80.3	0.5007	-	91.5	0.5007	-
50.1	0.6000	-	62.3	0.6000	-	75.5	0.6000	-	89.4	0.6000	-	103.5	0.6000	-
51.3	0.7515	-	64.5	0.7515	-	80.2	0.7515	-	97.5	0.7515	-	115.7	0.7515	-
51.8	0.8445	-	64.5	0.8445	-	80.8	0.8445	-	99.4	0.8445	-	119.0	0.8445	-
52.8	0.9393	-	66.4	0.9393	-	82.5	0.9393	-	100.0	-	0.9393	117.8	-	0.9393
54.9	0.9602	-	69.4	0.9602	-	84.5	0.9602	-	99.1	-	0.9602	112.2	-	0.9602
55.2	0.9701	-	70.5	0.9701	-	84.1	-	0.9701	95.9	-	0.9701	104.4	-	0.9701

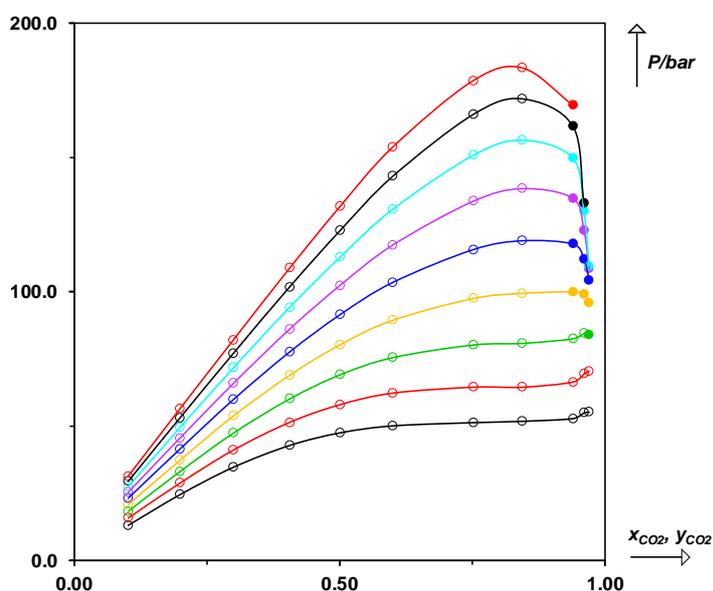| T/K = 343.15			T/K = 353.15			T/K = 363.15			T/K = 373.15		
P/bar	x_{CO_2}	y_{CO_2}	P/bar	x_{CO_2}	y_{CO_2}	P/bar	x_{CO_2}	y_{CO_2}	P/bar	x_{CO_2}	y_{CO_2}
25.4	0.1014	-	27.5	0.1014	-	29.5	0.1014	-	31.4	0.1014	-
45.6	0.1990	-	49.5	0.1990	-	53.1	0.1990	-	56.5	0.1990	-
65.9	0.2996	-	71.7	0.2996	-	77.1	0.2996	-	82.1	0.2996	-
86.1	0.4055	-	94.2	0.4055	-	101.8	0.4055	-	108.8	0.4055	-
102.4	0.5007	-	112.9	0.5007	-	122.8	0.5007	-	131.8	0.5007	-
117.4	0.6000	-	130.7	0.6000	-	143.0	0.6000	-	153.9	0.6000	-
133.7	0.7515	-	150.8	0.7515	-	166.0	0.7515	-	178.6	0.7515	-
138.4	0.8445	-	156.4	0.8445	-	171.8	0.8445	-	183.3	0.8445	-
134.8	-	0.9393	149.8	-	0.9393	161.7	-	0.9393	169.5		0.9393
122.8	-	0.9602	130.0	-	0.9602	133.0	-	0.9602			
108.7	-	0.9701	109.6	-	0.9701						

Figure 1. Isothermal (P,x,y) cross-sections for the system CO_2 + cyclooctane at temperatures ranging from 293.15 K to 373.15 K with a step of 10 K. ○: experimental bubble point. ●: experimental dew point. The continuous line simply connects the experimental data points through spline functions.

4. Modeling and discussion

Before correlating the measured data with the Peng-Robinson EoS armed with sophisticated mixing rules, it is important to notice that at $T_2 = 303.15$ K, the experimentally measured bubble curve exhibits a horizontal plateau: for compositions 0.7515 and 0.8445, the measured bubble pressures are exactly the same ($P_{bubble} = 64.5$ bar). The presence of this horizontal plateau strongly suggests – at these specific temperature and pressure (T/K = 303.15 and P/bar = 64.5) – the existence of a lower critical end point ($LCEP_{LL}$), i.e., of an equilibrium between a vapor phase and a liquid–liquid critical point [23] (the liquid–liquid critical composition is somewhere between 0.7515 and 0.8445). Let us indeed recall that a CEP_{LL} is characterized by the simultaneous presence of an inflection point and a horizontal tangent on the bubble curve (refer to Fig. 20 (panel e) in [23] for more details) so that the bubble curve necessarily exhibits a horizontal plateau in the immediate vicinity of the CEP composition. In other words, a 3-phase line is presumably born at $T_2 = 303.15$ K. The temperature range in which such a 3-phase line exists seems to be very narrow since for temperatures ranging from 323 to 373 K, *classical* phase behaviors (as those observed in type I systems of the classification scheme of Van Konynenburg and Scott [23,24]) are observed. At 313.15 K, the existence of very close bubble-point pressures at $x_{co2} = 0.75$ and 0.84 is compatible with the presence of a liquid-liquid region above a 3-phase line. In such a case, the 2 measured points for $x_{co2} = 0.75$ and 0.84 would not be truly bubble points like the others since they would correspond to the disappearance of a liquid phase. It is however worth recalling that adjectives "liquid" and "gas" lose their common sense in the critical region. The simultaneous presence of a liquid-vapor critical point (at around 84.6 bar for a mole fraction of about 0.965) leads one to believe that the CO_2 + cyclooctane binary system exhibits a type V (or IV) behavior in the classification proposed by Van Konynenburg and Scott. However, it is important to emphasize that no liquid-liquid-vapor equilibrium was observed during our experiments so that we cannot exclude that the CO_2 + cyclooctane is a type I binary system. This lack of formal conclusion is due to the very narrow domain of existence of the probable three-phase line and to the lack of experimental data in this region. Undoubtedly, more experiments would be required in order to confirm the occurrence of LLVE and the type of phase behavior.

It was thus a challenge to check if cubic EoS armed with sophisticated mixing rules could reproduce such a type V phase behavior. In this study, it was decided to select the PR EoS in order to represent the thermodynamics of the CO_2 + cyclooctane system:

$$P(T,v,z) = \frac{R \cdot T}{v - b_m} - \frac{a_m}{v(v + b_m) + b_m(v - b_m)} \tag{1}$$

Two sets of mixing rules were used:

- **_SET 1:_** Classical van der Waals mixing rules with temperature-dependent binary interaction parameters ($k_{ij}(T)$):

$$\begin{cases} b_m = \displaystyle\sum_{i=1}^{NC} z_i b_i \\ a_m = \displaystyle\sum_{i=1}^{NC}\sum_{j=1}^{NC} z_i z_j \sqrt{a_i a_j}\left(1 - k_{ij}(T)\right) \end{cases} \tag{2}$$

With:

$$k_{ij}(T) = \frac{A_{ij} \cdot \left(\dfrac{298.15}{T}\right)^{\left(\frac{B_{ij}}{A_{ij}} - 1\right)} - \left(\dfrac{\sqrt{a_i(T)}}{b_i} - \dfrac{\sqrt{a_j(T)}}{b_j}\right)^2}{2\dfrac{\sqrt{a_i(T) \cdot a_j(T)}}{b_i \cdot b_j}} \tag{3}$$

Such mixing rules are those used in the well-established PPR78 model [25,26]. In the latter model, a group-contribution method was especially developed to calculate the 2 parameters A_{ij} and B_{ij}. In this study, they were fitted to experimental data in order to minimize the mean absolute deviations, at specified temperature and pressure, between calculated and experimental liquid phase and gas phase compositions. This is indeed the objective function which was systematically used during the development of the PPR78 model. The optimal values were found to be: $A_{12} = 144.3\ MPa$ and $B_{12} = 407.6\ MPa$.

- **_SET 2:_** Advanced mixing rules that combine the residual part of the Wilson [27] activity coefficient model ($a_{residual}^{E,Wilson} = a^{E,Wilson} - a_{combinatorial}^{E,Wilson}$) and the PR EoS:

$$
\begin{cases}
b_m = \sum_{i=1}^{NC}\sum_{j=1}^{NC} z_i z_j b_{ij} \quad \text{with: } b_{ij} = \left(\dfrac{b_i^{2/3} + b_j^{2/3}}{2}\right)^{3/2} \\[2ex]
\dfrac{a_m}{b_m} = \sum_{i=1}^{NC} z_i \dfrac{a_i}{b_i} + \dfrac{a_{residual}^{E,Wilson}}{\Lambda} \quad \text{with: } \Lambda = \dfrac{-\sqrt{2}}{2}\ln\left(1+\sqrt{2}\right) \approx -0.6232 \text{ and:} \\[2ex]
a_{residual}^{E,Wilson}(T,\boldsymbol{x}) = \underbrace{\left\{ -x_1 \ln\left[x_1 + x_2\dfrac{b_2}{b_1}\exp\left(-\dfrac{A_{12}}{T}\right)\right] - x_2 \ln\left[x_2 + x_1\dfrac{b_1}{b_2}\exp\left(-\dfrac{A_{21}}{T}\right)\right]\right\}}_{a^{E,Wilson}} \\[3ex]
\qquad\qquad\quad - \underbrace{\left[x_1 \ln\left(\dfrac{b_1}{x_1 b_1 + x_2 b_2}\right) + x_2 \ln\left(\dfrac{b_2}{x_1 b_1 + x_2 b_2}\right)\right]}_{a_{combinatorial}^{E,Wilson}}
\end{cases}
\tag{4}
$$

Such mixing rules (MR) can be seen as a mix between Huron-Vidal [28] MR and those used in the UMR-PRU [29–33] model. Here also, the two parameters A_{12} and A_{21} were fitted to experimental data. The optimal values that minimize the deviations between calculated and experimental phase compositions are: $A_{12} = 309.4\ K$ and $A_{21} = 4.566\ K$.

In all cases, pure-component parameters (a_i and b_i) were classically calculated by:

$$
\begin{cases}
a_i(T) = a_{c,i} \cdot \alpha_i(T) \\[1ex]
\alpha_i(T) = \left[1 + m_i\left(1 - \sqrt{T/T_{c,i}}\right)\right]^2 \\[1ex]
m_i = 0.37464 + 1.54226\omega_i - 0.26992\omega_i^2 \\[1ex]
a_{c,i} = \Omega_a \cdot \dfrac{R^2 T_{c,i}^2}{P_{c,i}} \\[1ex]
b_i = \Omega_b \cdot \dfrac{R T_{c,i}}{P_{c,i}} \\[1ex]
X = \left[1 + \sqrt[3]{4 - 2\sqrt{2}} + \sqrt[3]{4 + 2\sqrt{2}}\right]^{-1} \approx 0.25308 \\[1ex]
\Omega_a = \dfrac{8 + 40X}{49 - 37X} \approx 0.45724 \\[1ex]
\Omega_b = \dfrac{X}{X+3} \approx 0.07780
\end{cases}
\tag{5}
$$

Pure-component properties (experimental critical temperature, $T_{c,i}$, pressure, $P_{c,i}$, and acentric factor, ω_i) considered in this work stem from the DIPPR database. In this study, the Soave [34] α-function was selected because, as shown in [35–37], it holds the

thermodynamically consistent *positive - monotonically decreasing - convex* behavior, within the temperature domain that characterizes the phase-equilibrium data acquired in this study.

4.1. Discussion on the correlation of the measured data with the PR EoS armed with classical van der Waals mixing rules and temperature-dependent binary interaction parameters

Fig. 2 highlights that the classical VdW mixing rules with temperature-dependent binary interaction parameters predict a type III phase diagram meaning that non-experimentally-observed three-phase lines are predicted at low temperatures (293 and 303 K) as shown in Fig. 3. With this first set of mixing rules (see Fig. 3), dew-point pressures are predicted with high accuracy. Apart from the critical region, bubble-point pressures tend to be underestimated by the model. The critical region is particularly difficult to reproduce here because the temperatures at which the measurements were performed are slightly above that of the calculated UCEP (T_{UCEP} = 316 K). In this region (see in particular the calculated isothermal phase diagrams at 323 and 333 K), the disappearance of the three-phase line distorts the isothermal phase diagrams by inducing the presence of inflection points on the bubble curve which makes extremely difficult a faithful reproduction of the data. Even if this first set of mixing rules does not predict – as experimentally suspected – a type V (or IV) phase diagram, it would be unfair to conclude that such mixing rules are not able to correlate complex systems. Indeed, it is known by experience that a very small number of binary systems exhibit a type V (or IV) phase diagram. As an example, in the homologous series of mixtures containing CO_2 and a *n*-alkane, a type IV is only observed for the system CO_2 + *n*-C_{13} whereas mixtures of CO_2 with *n*-C_{14} or with longer *n*-alkanes exhibit type III phase behavior. Type V (or IV) phase diagrams are thus ephemeral and by slightly modifying the parameters of the EoS, we move from a type IV to a type III phase behavior. In other words, it is really scarce to predict a type IV phase behavior with an EoS.
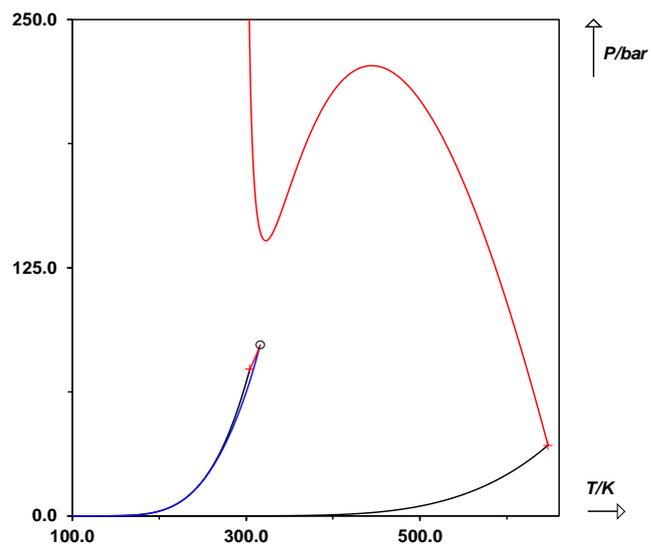
Figure 2. Type III *Global Phase Equilibrium Diagram* (as named by Cismondi and Michelsen [38,39]) of the CO_2 + cyclooctane binary system as predicted by the PR EoS armed with classical VdW mixing rules and temperature-dependent binary interaction parameters.
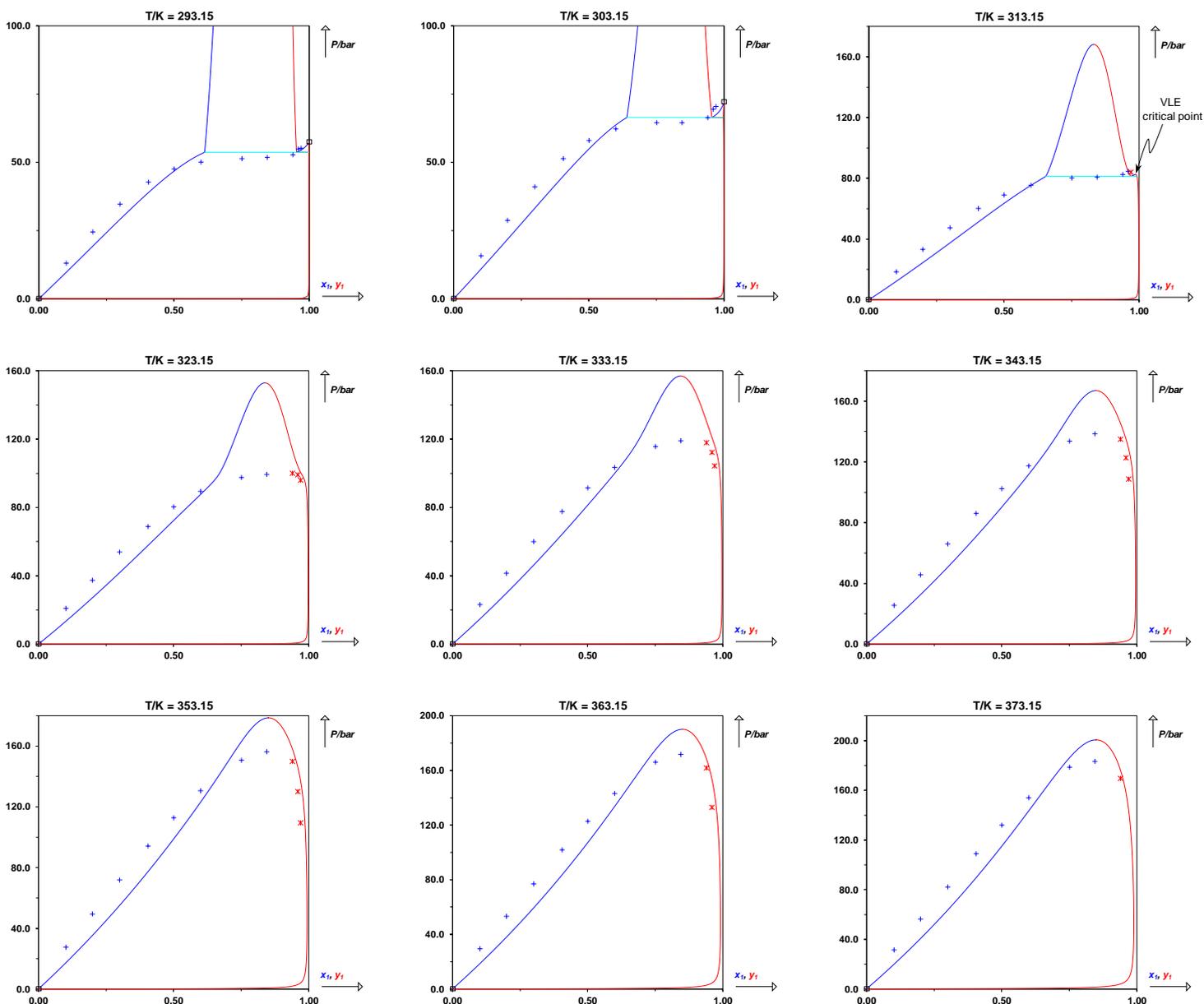
Figure 3. Correlation of the fluid-phase equilibrium data measured in this study (see Table 2) with the PR EoS armed with classical VdW mixing rules and temperature-dependent binary interaction parameters. **+**: experimental bubble point. **∗**: experimental dew point.

4.2. Discussion on the correlation of the measured data with the PR EoS armed with advanced mixing rules that embed the residual part of the Wilson activity coefficient model

As shown in Figs. 4 and 5, such mixing rules predict a type V phase behavior and make it possible to reproduce the correct topology of the studied binary system. In particular, the model does not predict a three-phase line at 293.15 and 303.15 K. The calculated temperature of the LCEP (T_{LCEP} = 306.15 K) is only 3 K above the alleged experimental value. Moreover,

at $T_3 = 313.15$ K, it is noticeable that the model predicts with high accuracy the temperature, pressure and composition of the VLE critical point. The unique deficiency of the model is the poor prediction – at temperatures above 313.15 K – of bubble-point pressures for the 2 compositions ($x_1 = 0.7515$ and $x_1 = 0.8445$) that felt in the liquid-liquid region at 313.15 K. As previously stated, this is the consequence of the disappearance of the 3-phase line that causes inflection points to appear on the bubble curve.
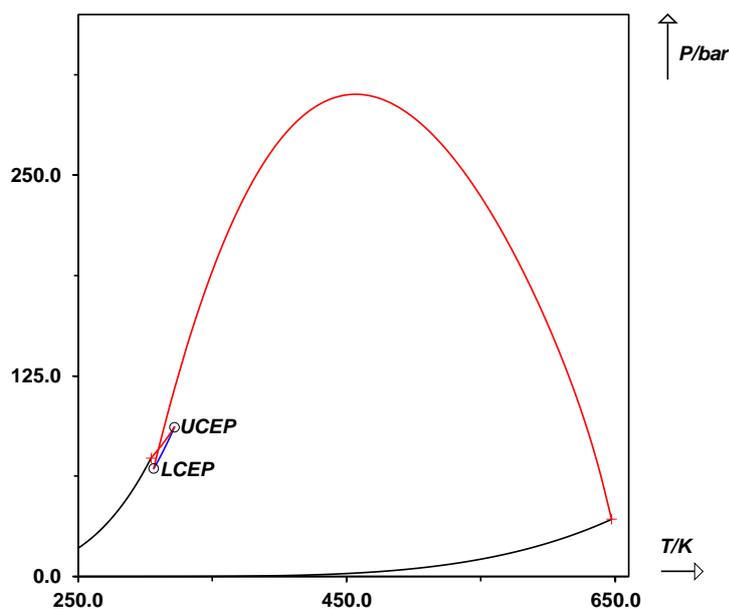

Figure 4. Type V *Global Phase Equilibrium Diagram* (GPED) of the CO_2 + cyclooctane binary system as predicted by the PR EoS armed with advanced mixing rules that embed the residual part of the Wilson activity coefficient model.
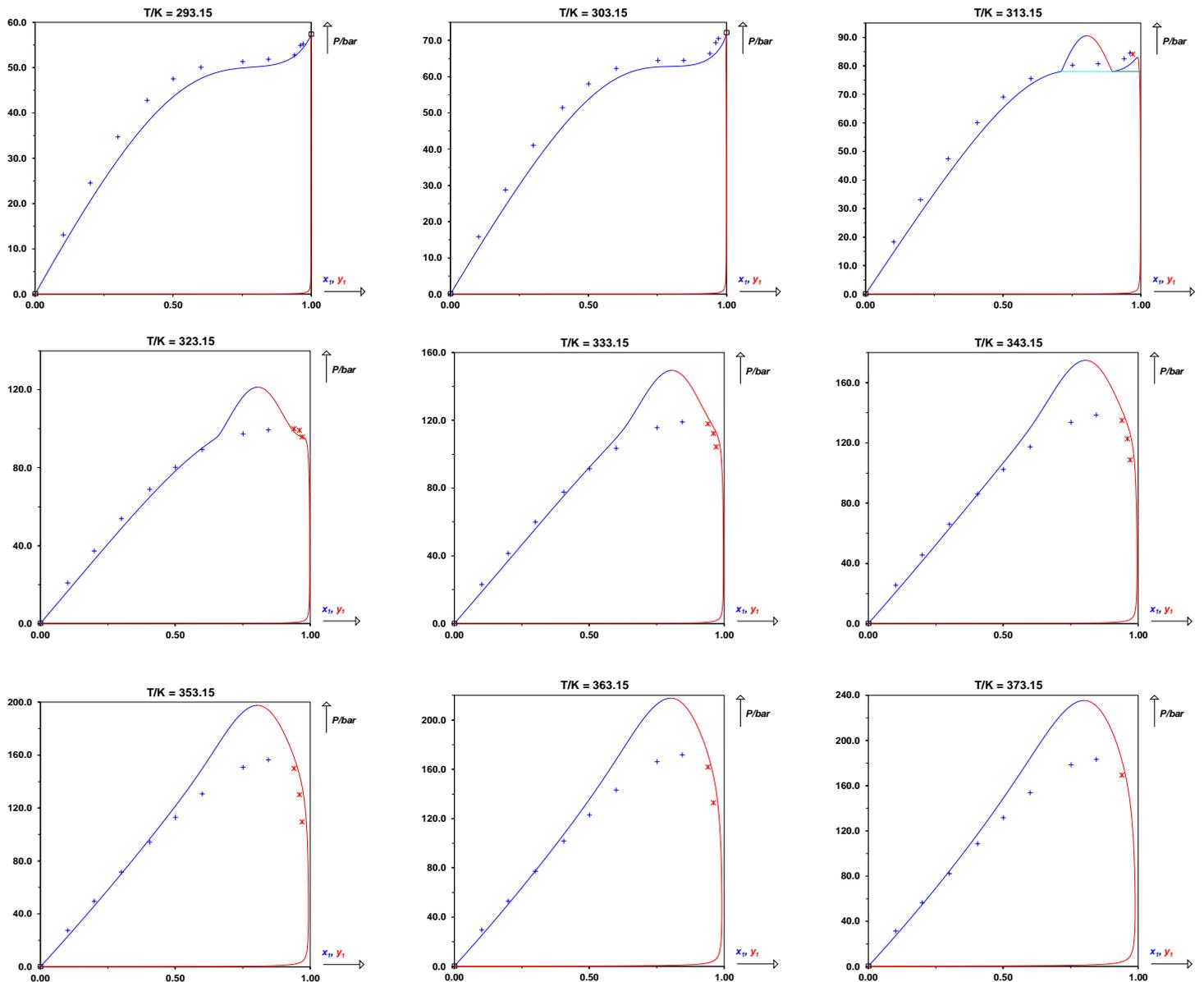
Figure 5. Correlation of the fluid-phase equilibrium data measured in this study (see Table 2) with the PR EoS armed with advanced mixing rules that embed the residual part of the Wilson activity coefficient model. +: experimental bubble point. ∗ : experimental dew point.

5. Conclusion

Using a high-pressure variable volume cell, bubble- and dew-point pressures of the CO_2 + cyclooctane binary system were measured for 11 different global compositions in a temperature range varying between 292.95 and 373.55 K. A total of 96 experimental data points, ranging from 13.2 to 183.4 bar, were measured.

The main conclusion of this investigation is that the studied binary system either exhibits a type I or a type V phase behavior in the classification scheme of Van Konynenburg and Scott. It was indeed experimentally observed that at 303.15 K, two mixtures with very different global compositions (0.7515 and 0.8445) have exactly the same bubble-point pressure (P = 64.5 bar). Starting from this observation, 2 possibilities arise:

1. we could argue that considering the experimental uncertainty, these two bubble-point pressures are not exactly identical and that the measured bubble-point pressure at x=0.8445 is in fact slightly higher than that at x=0.7515. In such a case, we have to conclude that the CO_2 + cyclooctane system is a type-I system in the classification scheme of Van Konynenburg and Scott.

2. It is assumed that the two bubble-point pressures are identical what makes necessarily appear an inflexion point with a horizontal tangent on the bubble curve which is the characteristic of a critical end point. In other words, a 3-phase line starts or ends at 303.15 K. However, the measured phase diagram at 293.15 K clearly indicates that there is no 3-phase line at this temperature (the bubble-curve is a monotonically increasing function of composition). We can therefore conclude that a 3-phase line is born at 303.15 K. The critical end point is therefore a lower critical end point so that the CO_2 + cyclooctane system exhibits a type V phase behavior.

Both possibilities are perfectly admissible but more experiments are necessary to confirm the type of phase behavior. It is however believed that a new type V system was discovered. Indeed at 313.15 K, the two measured bubble-point pressures for x=0.7515 and x=0.8445 are still very close (80.2 and 80.8 bar) what is totally compatible with the presence of a fluid-fluid 2-phase region (above the 3-phase line) in this composition range.

Although the complexity of the phase behavior, the experimental data could be satisfactorily correlated with the Peng-Robinson equation of state coupled with sophisticated mixing rules. In particular, the Huron-Vidal-Wilson mixing rule, coupled with a quadratic mixing rule for the covolume were able to predict a type V phase diagram with a LCEP temperature only 3 K above the alleged experimental value. It is believed that such mixing rules that only use 2 parameters are among the most versatile ones

Experimental determination and modelling of high-pressure phase behavior for the binary system CO_2 + cyclooctane

References

[1] J.M.S. Fonseca, R. Dohrn, S. Peper, High-pressure fluid-phase equilibria: Experimental methods and systems investigated (2005–2008), Fluid Phase Equilibria. 300 (2011) 1–69. https://doi.org/10.1016/j.fluid.2010.09.017.

[2] S. Peper, J.M.S. Fonseca, R. Dohrn, High-pressure fluid-phase equilibria: Trends, recent developments, and systems investigated (2009–2012), Fluid Phase Equilibria. 484 (2019) 126–224. https://doi.org/10.1016/j.fluid.2018.10.007.

[3] P. Theveneau, X. Xu, O. Baudouin, J.-N. Jaubert, P. Ceragioli, C. Coquelet, Vapor–liquid equilibria of the $CH_4 + CO_2 + H_2S$ ternary system with two different global compositions: experiments and modeling, J. Chem. Eng. Data. 65 (2020) 1802–1813. https://doi.org/10.1021/acs.jced.9b01082.

[4] C. Latsky, C.E. Schwarz, High pressure vapor–liquid equilibrium data for the quaternary carbon dioxide + 1-decanol + 3,7-dimethyl-1-octanol + *n*-dodecane system, J. Chem. Eng. Data. 64 (2019) 5785–5796. https://doi.org/10.1021/acs.jced.9b00740.

[5] C. Latsky, N.S. Mabena, C.E. Schwarz, High pressure phase behaviour for the CO_2 + n-dodecane + 3,7-dimethyl-1-octanol system, The Journal of Supercritical Fluids. 149 (2019) 138–150. https://doi.org/10.1016/j.supflu.2019.04.002.

[6] C. Latsky, B. Cordeiro, C.E. Schwarz, High pressure bubble- and dew-point data for systems containing CO_2 with 1-decanol and n-hexadecane, Fluid Phase Equilibria. 521 (2020) 112702. https://doi.org/10.1016/j.fluid.2020.112702.

[7] J.-N. Jaubert, P. Borg, L. Coniglio, D. Barth, Phase equilibria measurements and modeling of EPA and DHA ethyl esters in supercritical carbon dioxide, Journal of Supercritical Fluids. 20 (2001) 145–155. https://doi.org/10.1016/S0896-8446(01)00062-6.

[8] Y. Gao, C. Li, S. Xia, P. Ma, Estimation and correlation of phase equilibrium of CO_2 – hydrocarbon systems with PRMHV2-UNIFAC and PRMHV2-NRTL models, J. Chem. Eng. Data. 65 (2020) 655–663. https://doi.org/10.1021/acs.jced.9b00890.

[9] J. Wang, X. Yuan, H. Zhao, Y. Wang, X. Zhu, X. Guo, J.-N. Jaubert, Thermophysical properties of switchable-hydrophilicity solvent systems: N,N-Dipropyl-1-propanamine, water and carbon dioxide, The Journal of Chemical Thermodynamics. 143 (2020) 106049. https://doi.org/10.1016/j.jct.2020.106049.

[10] S.ZS. Al Ghafri, J.P.M. Trusler, Phase equilibria of (Methylbenzene + Carbon dioxide + Methane) at elevated pressure: Experiment and modelling, The Journal of Supercritical Fluids. 145 (2019) 1–9. https://doi.org/10.1016/j.supflu.2018.11.012.

[11] S. Vitu, R. Privat, J.-N. Jaubert, F. Mutelet, Predicting the phase equilibria of CO_2 + hydrocarbon systems with the PPR78 model (PR EoS and k_{ij} calculated through a group contribution method), Journal of Supercritical Fluids. 45 (2008) 1–26. https://doi.org/10.1016/j.supflu.2007.11.015.

[12] S. Sima, J.M. Milanesio, J.I. Ramello, M. Cismondi, C. Secuianu, V. Feroiu, D. Geană, The effect of the naphthenic ring on the VLE of (carbon dioxide + alkane) mixtures, The Journal of Chemical Thermodynamics. 93 (2016) 374–385. https://doi.org/10.1016/j.jct.2015.07.018.

[13] R.J. Wilcock, R. Battino, E. Wilhelm, The solubility of gases in liquids 10. The solubility of He, Ne, Ar, Kr, N2, O2, CO, CO2, CH4, CF4, and SF6 in cyclooctane at 289 to 313 K, The Journal of Chemical Thermodynamics. 9 (1977) 111–115. https://doi.org/10.1016/0021-9614(77)90075-1.

[14] S. Vitu, J.-N. Jaubert, F. Mutelet, Extension of the PPR78 model (Predictive 1978, Peng-Robinson EoS with temperature-dependent k_{ij} calculated through a group contribution method) to systems containing naphtenic compounds, Fluid Phase Equilibria. 243 (2006) 9–28. https://doi.org/10.1016/j.fluid.2006.02.004.

[15]   D.-Y. Peng, D.B. Robinson, A new two-constant equation of state, Industrial & Engineering Chemistry Fundamentals. 15 (1976) 59–64. https://doi.org/10.1021/i160057a011.

[16]   A. Pina-Martinez, R. Privat, J.-N. Jaubert, D.-Y. Peng, Updated versions of the generalized Soave α-function suitable for the Redlich-Kwong and Peng-Robinson equations of state, Fluid Phase Equilibria. 485 (2019) 264–269. https://doi.org/10.1016/j.fluid.2018.12.007.

[17]   S. Lasala, P. Chiesa, R. Privat, J.-N. Jaubert, VLE properties of CO_2–based binary systems containing N_2, O_2 and Ar: experimental measurements and modelling results with advanced cubic equations of state, Fluid Phase Equilibria. 428 (2016) 18–31. https://doi.org/10.1016/j.fluid.2016.05.015.

[18]   S. Lasala, P. Chiesa, R. Privat, J.-N. Jaubert, Measurement and prediction of multi-property data of CO_2-N_2-O_2-CH_4 mixtures with the "Peng-Robinson + residual Helmholtz energy-based" model, Fluid Phase Equilibria. 437 (2017) 166–180. https://doi.org/10.1016/j.fluid.2017.01.016.

[19]   S. Lasala, P. Chiesa, R. Privat, J.-N. Jaubert, Sizing and operating units for the purification and compression of CO_2-based streams: The impact of thermodynamic model accuracy, The Journal of Supercritical Fluids. 140 (2018) 336–347. https://doi.org/10.1016/j.supflu.2018.04.010.

[20]   S. Vitu, J.-N. Jaubert, J. Pauly, J.-L. Daridon, D. Barth, Phase equilibria measurements of CO_2 + methyl cyclopentane and CO_2 + isopropyl cyclohexane binary mixtures at elevated pressures, Journal of Supercritical Fluids. 44 (2008) 155–163. https://doi.org/10.1016/j.supflu.2007.10.003.

[21]   S. Vitu, J.-N. Jaubert, J. Pauly, J.-L. Daridon, D. Barth, Bubble and dew points of carbon dioxide + a five-component synthetic mixture: experimental data and modeling with the PPR78 model, Journal of Chemical and Engineering Data. 52 (2007) 1851–1855. https://doi.org/10.1021/je7001978.

[22]   S. Vitu, J.-N. Jaubert, J. Pauly, J.-L. Daridon, High-pressure phase behaviour of the binary system CO_2 + cis-decalin from (292.75 to 373.75) K, Journal of Chemical Thermodynamics. 40 (2008) 1358–1363. https://doi.org/10.1016/j.jct.2008.05.008.

[23]   R. Privat, J.-N. Jaubert, Classification of global fluid-phase equilibrium behaviors in binary systems, Chemical Engineering Research and Design. 91 (2013) 1807–1839. https://doi.org/10.1016/j.cherd.2013.06.026.

[24]   P.H. Van Konynenburg, R.L. Scott, Critical Lines and Phase Equilibria in Binary Van Der Waals Mixtures, Philosophical Transactions of the Royal Society A: Mathematical, Physical and Engineering Sciences. 298 (1980) 495–540. https://doi.org/10.1098/rsta.1980.0266.

[25]   J.-N. Jaubert, F. Mutelet, VLE predictions with the Peng-Robinson equation of state and temperature-dependent k_{ij} calculated through a group contribution method, Fluid Phase Equilibria. 224 (2004) 285–304. https://doi.org/10.1016/j.fluid.2004.06.059.

[26]   J.-W. Qian, J.-N. Jaubert, R. Privat, Phase equilibria in hydrogen-containing binary systems modeled with the Peng-Robinson equation of state and temperature-dependent binary interaction parameters calculated through a group-contribution method, Journal of Supercritical Fluids. 75 (2013) 58–71. https://doi.org/10.1016/j.supflu.2012.12.014.

[27]   G.M. Wilson, Vapor-liquid equilibrium. XI. A new expression for the excess free energy of mixing, J. Am. Chem. Soc. 86 (1964) 127–130. https://doi.org/10.1021/ja01056a002.

[28]   M.-J. Huron, J. Vidal, New mixing rules in simple equations of state for representing vapour-liquid equilibria of strongly non-ideal mixtures, Fluid Phase Equilibria. 3 (1979) 255–271. https://doi.org/10.1016/0378-3812(79)80001-1.

[29]   E. Voutsas, K. Magoulas, D. Tassios, Universal mixing rule for cubic equations of state applicable to symmetric and asymmetric systems: results with the Peng−Robinson equation of state, Industrial & Engineering Chemistry Research. 43 (2004) 6238–6246. https://doi.org/10.1021/ie049580p.

[30]   E. Voutsas, V. Louli, C. Boukouvalas, K. Magoulas, D. Tassios, Thermodynamic property calculations with the universal mixing rule for EoS/G^E models: Results with the Peng–Robinson EoS and a UNIFAC model, Fluid Phase Equilibria. 241 (2006) 216–228. https://doi.org/10.1016/j.fluid.2005.12.028.

[31]   V. Louli, G. Pappa, C. Boukouvalas, S. Skouras, E. Solbraa, K.O. Christensen, E. Voutsas, Measurement and prediction of dew point curves of natural gas mixtures, Fluid Phase Equilibria. 334 (2012) 1–9. https://doi.org/10.1016/j.fluid.2012.07.028.

[32]   G.D. Pappa, C. Perakis, I.N. Tsimpanogiannis, E.C. Voutsas, Thermodynamic modeling of the vapor–liquid equilibrium of the CO2/H2O mixture, Fluid Phase Equilibria. 284 (2009) 56–63. https://doi.org/10.1016/j.fluid.2009.06.011.

[33]   E.G. Petropoulou, E.C. Voutsas, Thermodynamic modeling and simulation of natural gas dehydration using triethylene glycol with the UMR-PRU model, Ind. Eng. Chem. Res. 57 (2018) 8584–8604. https://doi.org/10.1021/acs.iecr.8b01627.

[34]   G. Soave, Equilibrium constants from a modified Redlich-Kwong equation of state, Chemical Engineering Science. 27 (1972) 1197–1203. https://doi.org/10.1016/0009-2509(72)80096-4.

[35]   Y. Le Guennec, S. Lasala, R. Privat, J.-N. Jaubert, A consistency test for α-functions of cubic equations of state, Fluid Phase Equilibria. 427 (2016) 513–538. https://doi.org/10.1016/j.fluid.2016.07.026.

[36]   Y. Le Guennec, R. Privat, S. Lasala, J.-N. Jaubert, On the imperative need to use a consistent α-function for the prediction of pure-compound supercritical properties with a cubic equation of state, Fluid Phase Equilibria. 445 (2017) 45–53. https://doi.org/10.1016/j.fluid.2017.04.015.

[37]   Y. Le Guennec, R. Privat, J.-N. Jaubert, Development of the translated-consistent *tc*-PR and *tc*-RK cubic equations of state for a safe and accurate prediction of volumetric, energetic and saturation properties of pure compounds in the sub- and super-critical domains, Fluid Phase Equilibria. 429 (2016) 301–312. https://doi.org/10.1016/j.fluid.2016.09.003.

[38]   M. Cismondi, M.L. Michelsen, Global phase equilibrium calculations: Critical lines, critical end points and liquid–liquid–vapour equilibrium in binary mixtures, The Journal of Supercritical Fluids. 39 (2007) 287–295. https://doi.org/10.1016/j.supflu.2006.03.011.

[39]   M. Cismondi, M. Michelsen, Automated calculation of complete Pxy and Txy diagrams for binary systems, Fluid Phase Equilibria. 259 (2007) 228–234. https://doi.org/10.1016/j.fluid.2007.07.019.